JOURNAL OF MATERIALS SCIENCE **37** (2002) 177–183

Spectroscopic and thermal contribution to the structural characterization of vandenbrandeite

I. L. BOTTO*, V. L. BARONE
Centro de Química Inorgánica (CEQUINOR-CONICET), Facultad de Ciencias Exactas, Universidad Nacional de La Plata, La Plata (1900) Argentina
E-mail: botto@dalton.quimica.unlp.edu.ar

M. A. SANCHEZ
CINDECA and CICPBA, La Plata (1900) Argentina

The vibrational (IR and Raman) spectrum of Vandenbrandeite, $Cu[UO_2(OH)_4]$, has been recorded and discussed on the basis of structural considerations through the use of empirical expressions. As the H-bonding in the lattice is poorly known, the characteristics of this bond has been analyzed with the aid of H/D isotope exchange, thermal assays and electron microscopy. Samples are practically amorphous to XRD up to ~700°C whereas crystals morphologically different by SEM microscopy and well characterized by XRD technique are observed from ~800°C. Vibrational spectroscopy reveals that the atomic arrangement in the structure remains largely unaffected as the dehydration proceeds, suggesting a topochemically controlled process. EPR spectroscopy suggests a disordered distribution of Cu(II) ions as temperature increases. Finally, thermal dehydroxylation and paragenesis of the copper-uranyl oxide hydrate are correlated.

1. Introduction

Vandenbrandeite, the $Cu[UO_2(OH)_4]$ hydrous copper uranate, is a very rare mineral species that like another uranyl oxide hydrates (UOHs), appears as an alteration product of uraninite. All the known structures of the UOHs are based on structural sheet of edge sharing polyhedra containing the U(VI) ion. The topology of the UOH structural layers is remarkably similar to that of the U_3O_8 oxide [1].

The crystallography of the dark green mineral was analyzed by Milne and Nuffield [2] whereas Rozenzweig and Ryan have determined the crystal structure [3]. This basically consists of layers formed by $[Cu_2O_6]$ and $[U_2O_{12}]$ interconnected units [3]. The U environment shows five U—O bonds in a pentagonal plane and two shorter ones, characteristic of the uranyl group. The Cu-polyhedron is approximately square pyramidal. As the location of the H atoms in crystalline structures is usually unsatisfactory, except for studies based on neutron diffraction, the nature of the H-bond has been tentatively inferred by Rozenzweig and Ryan [3]. They suggested that the H atoms are associated to the equatorial oxygen atoms of the U-polyhedron (two U—O···H distances at 2.31 Å, two ones at 2.41 Å and the remaining one at 2.44 Å, proposing the $Cu[UO_2(OH)_4]$ formula (to replace the old $2CuO{\cdot}2UO_3{\cdot}5H_2O$ one [4]). Distances of the two shortest U—O bonds of the uranyl group are 1.77 and 1.78 Å respectively. The principal interactions between adjacent layers seem to be between these uranyl groups with the axial oxygen atoms of the Cu-square pyramids and through the hydrogen bonding associated to the oxygen atoms of the U-polyhedron. Hence, because the directional character of the O—H bonds, it seems to be nearer to a hydroxyl group than to a water molecule [3].

Although the IR spectrum of vandenbrandeite has been published, the vibrational spectrum has not been analyzed in detail [5].

In order to characterize this secondary uranium-mineral as well as to elucidate about the role of the H atoms in the lattice, the IR and Raman spectra of natural samples has been analyzed and discussed with the aid of additional assays such as thermal and H/D isotope exchange experiments. Thermal behavior has also been studied by means of infrared (IR) and electron spin resonance (ESR) spectroscopy, X-ray diffraction and scanning electron microscopy (SEM–EDAX). Thermal dehydroxylation and paragenesis of the studied UOH are correlated.

2. Experimental

The analyzed specimen is original from the Kalongwe deposit, Shaba, province of Zaire and was kindly provided by Prof. M. Deliens from the Institute Royal des Sciences naturelles de Belgique (Bruxelles, Belgium) [6].

The material is mainly associated to the ochre-yellow mineral kasolite ($PbUO_2SiO_4{\cdot}H_2O$), also product of

*Author to whom all correspondence should be addressed.

alteration of uraninite. Thin veinlets of kasolite are randomly located within the massive green tabular crystals of vandenbrandeite [7].

Preliminary elimination of impurities was carried out washing and stirring with a mixture of water and acetone. No alteration of green crystals has been observed after this treatment. Although the bigger crystals show inclusions of kasolite, difficult to eliminate by washing, it has been possible to select carefully small and pure crystals of vandenbrandeite.

The chemical analysis of selected material, performed by electron microprobe (Philips 505 with energy dispersive detector EDAX-9100 electron microscopy instrument), reveals metallic contents of 21.00% of Cu and 79.00% of U (only traces of Pb and Si) in good agreement with the theoretical values (21.07% Cu and 78.93% U). Likewise, the yellow crystals of kasolite show the follow metal data: 43.3% Pb, 50.9% U and 5.8% Si, also in agreement with the theoretical values (43.78% Pb, 50.29% U and 5.93% Si).

The phase analysis was performed by X-ray diffractometry by means of a Philips PW 1714 diffractometer, Cu K_α radiation and Ni filter.

The IR spectra were recorded (4000–200 cm^{-1}) on a Perkin Elmer 580B spectrometer, using the KBr pellet and Nujol techniques. No difference in the IR spectra is observed. Spectra at liquid nitrogen temperature were obtained in the RIIC-VLT2 cell. The Raman spectrum was obtained with the Bruker IFS-66 equipment, laser Nd-YAG between 4000–100 cm^{-1}.

The X band electron spin resonance spectra (ESR) were recorded at room temperature (RT) on a Varian E-9 spectrometer equipped with an on-line computer for data treatment.

Partially deuterated samples were obtained by mixing the mineral with D_2O (99.9%) under hydrothermal treatment (150°C) during 7 days. However, only isotopically diluted samples were obtained. Further attempts to reach a greater deuteration were unsuccessful.

Thermal studies were carried out, on air, in a programmed temperature furnace between 300 and 950°C, using the DTA-TG literature data [5].

3. Results and discussion

$Cu[UO_2(OH)_4]$ belongs to the triclinic system with $a = 7.84$ Å, $b = 5.43$ Å, $c = 6.09$ A, $\alpha = 91°\ 52'$, $\beta = 102°\ 00'$, $\gamma = 89°\ 37'$, space group $P\bar{1}$ and $Z = 2$ (Ref. 3). On the basis of the existence of two types of heavy metals in the unit cell, the proton vibrations are very sensitive to the bonds to which are connected. Hence, U–O, Cu–O and H–O typical vibrations can be studied by means of IR and Raman spectroscopy (Fig. 1).

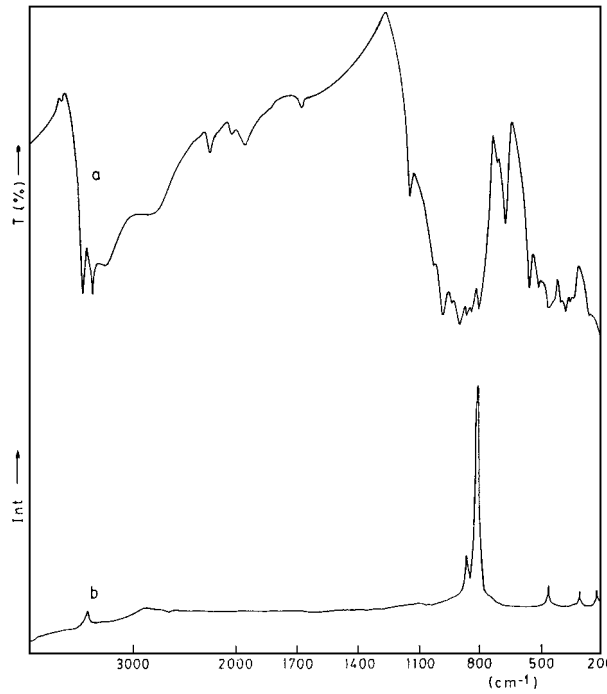

Figure 1 Vibrational spectrum of vandenbrandeite: (a) IR, (b) Raman.

3.1. The O–H vibrations

It is known that the H atom plays an important role in the structure and chemistry of oxides and other mineral species [8, 9]. The principal reason stems from the directional character of the chemical bonding in which H is involved.

IR spectroscopy has proved to be an important tool to study the presence of water and OH groups in mineral species. So, it is possible to establish unambiguously the difference between the water bands and those due to hydroxyl-groups [8, 10]. In relation to their assignment, a common region, between 3600–3000 cm^{-1} corresponds to the O–H stretching modes (depending on the degree of H-bonding), while a second region, close to 1600 cm^{-1}, is only attributable to H–O–H bending modes of water. A third region, below 900 cm^{-1}, can be assigned to OH and water librations [11, 12]. Likewise, the δM–O–H in plane bending vibrations, (M = metal atom with higher electronegativity), usually appear between 1100–800 cm^{-1} whereas the γM–O–H out of plane bending vibrations lie between 1000–500 cm^{-1} [5, 13]. A very weak IR-band in the 1600 cm^{-1} region could be attributed to the bending vibration of adsorbed water [5] although a series of another weak absorption bands in the 1300–2300 cm^{-1} corresponds to overtones and combinations as it is discussed above. In fact, the difference in the intensity between the bands in the 3500–3400 and 1600 cm^{-1} regions is the main support of the hydroxyl character of the H-bond in vandenbrandeite (in agreement with Rosenzweig and Ryan and more recently with Cejka [3, 5]).

However, a clearly resolved doublet in the IR spectrum, at 3508 and 3423 cm^{-1} suggest the presence of clearly distinguished kinds of hydroxyl entities. The sharp peaks located at the highest values of OH stretching region suggest a relatively "free" character of these groups [14]. The values are similar to those observed for strontium hydroxyde (3597–3496 cm^{-1}) or $Al(OH)_3$ (gibbsite) (3617, 3520, 3428, 3380 cm^{-1}) where very extensive H-bonds act as protons donors [10]. The additional broad band centered at 3262 cm^{-1} should be assigned to medium strength H-bonded (2.56 Å for the O···O hydrogen bonded distance of sharing edge dimeric U-unit [3]).

The bands located at 1139, 1024 and 978 cm^{-1} and those located in the 900 and 840 cm^{-1} region

are assigned to δU–O–H vibrations, as it is observed in metallic hydroxymetallates (Cu–O–H ($\sim$990 cm^{-1}) [14], U–O–H (1000–1100 cm^{-1}) [15], Te–O–H (1200–1100 cm^{-1}) [16]), M^{III}–O–H (M = Al, Fe, Ga, Sc) (1100–900 cm^{-1}) [10], Sn–O–H (1150–900 cm^{-1}) [17]).

The ability to form strong H-bonds is inherent to OH groups coordinated by metal atoms, depending on either feature of metal and steric considerations. So, in several copper hydroxyl sulfates the Cu–O–H IR-band is shifted from 990 to 734 cm^{-1} as the H-bond strength is decreased [14].

The third type of bands related to the OH groups (librational modes) appear below 700 cm^{-1} depending also on the nature of M–O–H bond. In general, an increase of covalence is accompanied by an increase of librational frequency [10].

The separation between H_2O and OH librations is performed by deuteration experiments due to HDO librations occur only in the case of water molecule [18].

In order to obtain a wider insight into the vibrational feature, the comparison between the IR spectra of original and partly deuterated sample has been shown in Figs 2a and b (4000–2000 cm^{-1}) and 3a and b (1200–200 cm^{-1}). They show the typical regions of OH or OD vibrations. The highest stretching modes are displaced to 2800–2500 cm^{-1} and a series of weak bands in the 2365–2330 cm^{-1} correspond to the shifting of the weaker OH bonds ($\sim$3200 cm^{-1}). Some changes are also observed in the middle region of the spectrum, where the U–O–H bands shift on deuteration to 849, 760 and 724 cm^{-1}, according to the Teller-Redlich rule [19]. In fact, the splitting of the band ($\sim$850 cm^{-1}) and a shoulder at 760 cm^{-1} account for this effect. Likewise, the supposition that the band at 842 cm^{-1} could be attributed to δU–O–H is corroborated by the presence of a weak band at 620 cm^{-1} in the spectrum of the deuterated sample. Finally, the O–D librational modes appear as very weak bands below 500 cm^{-1}, which practically overlaps the other vibrational modes at lower wavenumber. Table I gives the corresponding comparison.

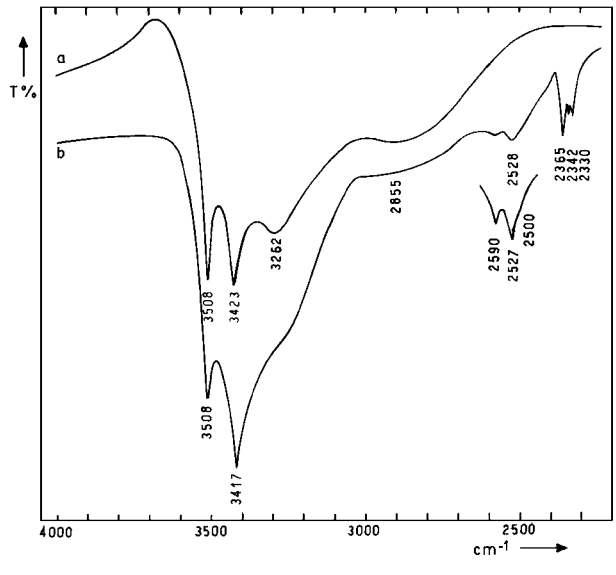

Figure 2 IR spectra of original (a) and partially deuterated (b) samples between 4000 and 2000 cm^{-1} (registered at LNT): OH and OD stretching modes.

TABLE I IR vibrations associated to the proton (in cm^{-1}). Comparison between the vibrations of the original and partially deuterated samples

Original sample	Deuterated sample	Assig.	$(\nu H)/(\nu D)$
3508	(3508), 2855	O–H	1.23
3423	(3417), 2590	and	1.32
3262	2527, 2500	O–D	1.29–1.30
2845	?	stretching	
$\sim$3100	2365		
	2342		$\sim$1.33
	2330		
1643		H_2O ?	
1139	(1122), 849	δU–O–H	1.34
1024	(1027), 760	and	1.34
978	(980), 724	δU–O–D	1.35
897	(895), 664		1.28
842	(849), 620		1.35
655	(656), 480	γU–O–H	1.36
		and	
		γU–O–D	
548	(550), 395		1.38
508	(508), 376		1.35
460	(455), 327		1.40
400	(395), 300		1.33

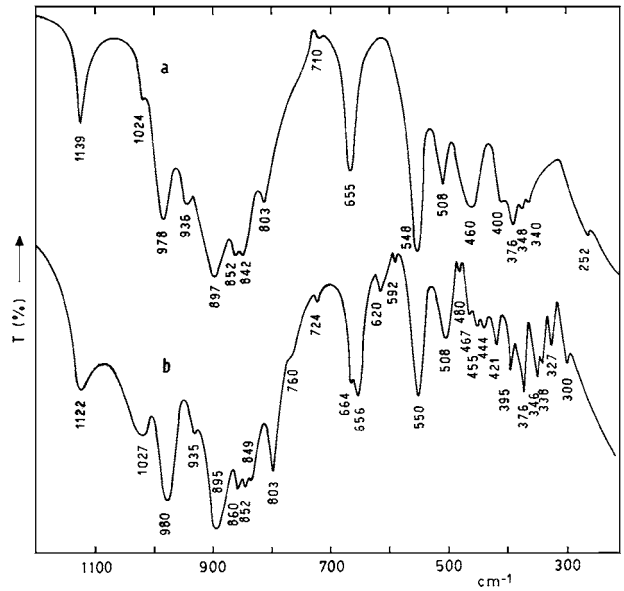

Figure 3 IR spectra of original (a) and partially deuterated (b) samples between 1200 and 200 cm^{-1} (registered at LNT): δU–O–H, δU–O–D modes and OH and OD librations.

Some empirical relations can be employed to estimate the O–H distances from spectroscopic data. Hence, the expression given by Hartert and Glemser [10] shows the relationship among the OH "effective anion radius" in Å, δU–O–H and ν_3 (OH):

$$d_{\text{O–H}} = 8.9 \times 10^{-4} \left[4720 - \delta\text{U–O–H} - 0.7\nu_{3(\text{OH})}\right] \quad (1)$$

The mean value of 1.11 Å is in agreement with data of related compounds [20].

On the other hand, the stronger H-bond may be that observed between two oxygen atoms of adjacent U polyhedron, for which correspond a O$\cdots$O distance of 2.56 Å (bond valence (s) $\sim$0.33 vu [21]). Such distance practically represents the minimum bond length observed in predicted bond valence (s) vs. O$\cdots$O distance curve, obtained from the fitting of a great number of

experimental data [21]. As the remaining equatorial O···O distances are higher than 2.56 Å, from geometrical considerations, it is clear the existence of, at least, two type of H bonds in the structure.

3.2. The U–O vibrations

According to the U–O bond-lengths in the U-polyhedron, it is possible to distinguish between the uranyl bonds (usually named $(U–O)_I$ and the equatorial ones $(UO)_{II}$ [10, 22, 23].

It is known that the uranyl ion usually has $D_{\infty h}$ linear symmetry. The ν_1 symmetric stretching mode, located between 700 and 900 cm^{-1} is Raman active but IR inactive. The ν_2 bending vibration and the ν_3 antisymmetric stretching mode located in the 350–200 cm^{-1} and in the 1000–850 cm^{-1} regions respectively, are IR allowed but Raman forbidden. A deviation from the linearity would lead to C_{2v} or to a lower symmetry and then, three non-degenerated vibrations should be observed (both IR and Raman active) [24, 25]. On the other hand, the equatorial $(U–O)_{II}$ bonds reveal typical absorption between 650 and 350 cm^{-1} [26, 27], although it seems to be more appropriate to relate the bands in this region to the presence of γU–O–H out of plane bending vibrations (506, 460 cm^{-1}) as well as to OH librational modes [5, 10].

The Raman spectrum of vandenbrandeite, shown in Fig. 1b, presents a sharp and very intense line at 805 cm^{-1}, assigned to the uranyl symmetric stretching. The IR band at 803 cm^{-1} is also attributed to this vibrational mode, activated in vandenbrandeite probably because the non-linearity of uranyl. Structural aspects of vandenbrandeite, not well discussed in literature, are surely responsible of this distortion, particularly the interaction between the layers (linking an axial coordination site of the copper square pyramid with an uranyl oxygen atom). The very intense IR band centered at 897 cm^{-1} as well as the weak Raman line at 862 cm^{-1} can be assigned to the uranyl antisymmetric stretching vibration. According to the Mc Glynn's expression and using the ν_1 value, the ν_3 position can be estimated (Ref. 28):

$$\nu_1 = 21 + 0.89\nu_3. \qquad (2)$$

The obtained value is 881 cm^{-1}. The position of this vibrational mode can be also calculated from the structural bond-lengths by means of empirical equations, such as:

$$d_{U–O} = 0.895 + 81.2\nu_3^{-2/3} \qquad (3) \quad \text{(Ref. 29)}$$

$$d_{U–O} = 0.975 + 74.75\nu_3^{-2/3} \qquad (4) \quad \text{(Ref. 30)}$$

$$d_{U–O} = 1.236 + 50.02\nu_3^{-2/3} \qquad (5) \quad \text{(Ref. 31)}$$

The obtained results ranging between 878 and 910 cm^{-1} confirm our assignment and are also in agreement with literature [9, 10, 32].

The position of the uranyl bending bands are related to the antisymmetric stretching values. Their wavenumbers gradually decrease as ν_3 increases [33]. Hence, ν_2 is expected at 250–200 cm^{-1} in the vandenbrandeite spectrum (252 cm^{-1}), though it is impossible to a more accurate assignment. A Raman line at 186 cm^{-1} (not shown in the figure) may be due to a vibrational motion of the group [34]. Additional weak bands associated to uranium usually appear at highest wavenumbers (2233, 2018 and 1946 cm^{-1}). They can be related to δU–O–H overtones and combinations [5, 25].

From the vibrational data, the UO_2^{++} estimated force constants are:

$$F_r = 6.31\ \text{mdyn/Å}$$

$$F_{rr} = -0.20\ \text{mdyn/Å}$$

where F_r is the stretching force constant while F_{rr} is the interaction constant [19]. These values are similar to those calculated from vibrational data of some uranyl compounds [35–37]. However, the negative value of F_{rr} implies weak attractive forces between the oxygen atoms and the partial non-validity of the linear symmetrical model. The U–O bond length of 1.75 Å estimated from the F_r constant by means of the Badger's rule [38]

$$\left(d_{U–O} = 1.08F_r^{-1/3} + 1.17\right) \qquad (6)$$

moderately agrees with structural information [3].

In relation to the Cu–O bonds, their vibrations are located below 500 cm^{-1} either in isolated polyhedron also in condensed systems [13, 39]. So, some band included in the group of them below 500 cm^{-1} in the IR spectrum and the Raman line at 474 cm^{-1} can be associated to the divalent metal.

3.3. Thermal behavior

TG and DTA plots of natural vandenbrandeite have been reported by Cejka [5]. The mineral shows endothermic signals between 390–395°C and 950–1025°C, whereas an exothermic signal is observed at ~550°C [5].

The greatest mass-loss is associated to dehydroxylation processes; in our samples it is observed in the range of 250–380°C (9.04%; theoretical mass loss = 8.96%)

The mineral continuously decomposes by further heating with a whole mass loss of ~10% at ~950°C.

The interpretation of the thermal process, given by Cejka [5] from combined DTA and TG results, suggests a first step of dehydroxylation, a second one of crystallization of oxides (CuU_3O_{10} and $CuUO_4$) and finally a series of not clear overlapped reactions, such as decompositions, phase transitions, sintering and melting [5]. Based on these results and specially due to the low crystallinity of the samples (in our case X-ray amorphous up to ~600°C), the thermal process has been analyzed by means of IR and ESR spectroscopies and SEM and EDAX microscopy.

Fig. 4 shows the comparative IR spectra of samples heated at 300, 600 and 950°C respectively and includes that of an untreated sample. It can be inferred that the dehydroxylation process takes place in steps, in agreement with the asymmetry of the DTA low-temperature signal, assuming a different type of H bonding in the structure. Although the intermediate product at 300 and 450°C are X-ray amorphous, the IR spectra are similar. They are related to those of U-oxides with a similar structural arrangement of U-polyhedron to that observed in vandenbrandeite. The spectra of UO_3 and U_3O_8 are showed in dashed line for comparative

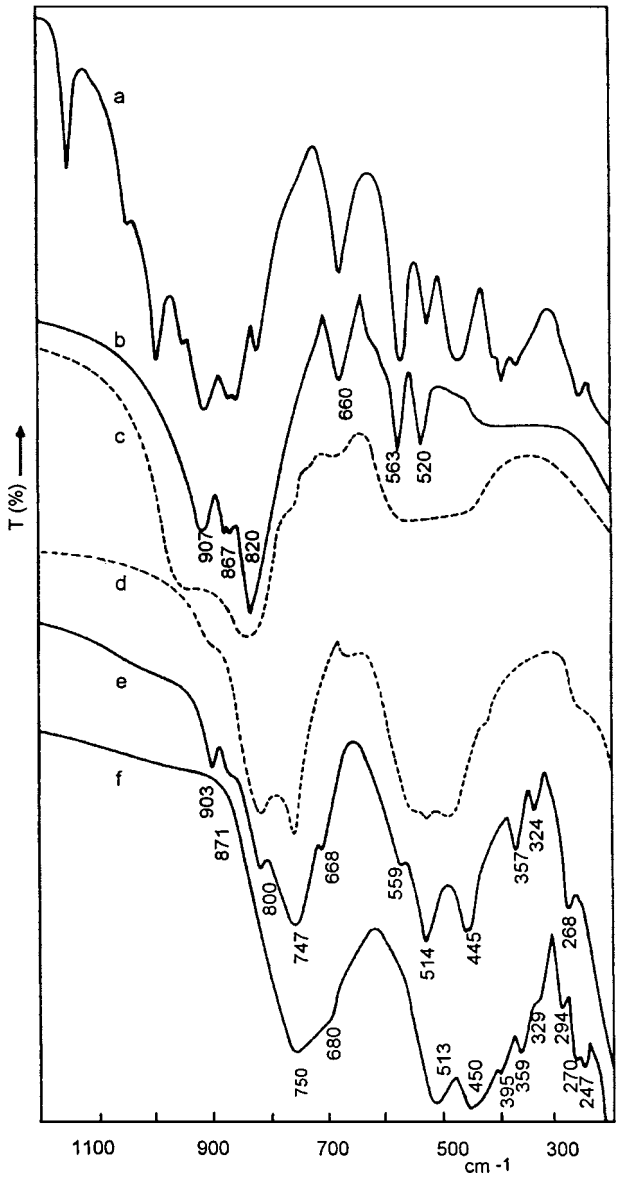

Figure 4 Comparative IR spectra in the course of thermal treatment (registered at RT) Original sample (a); mineral species heated up to 300°C (b); UO_3 as reference (c); U_3O_8 as reference (d); sample heated up to 600°C (e); sample heated up to 950°C (f).

purposes. The spectrum of the sample heated at 450°C (not shown in the figure) still shows a broad band (without splitting) in the O–H stretching region (centered at 3450 cm^{-1}) whereas no band in the OH bending region is observed. When the dehydroxylation is accomplished (600°C), the spectrum more clearly resembles to those of uranates, where the bands are attributed to $(U{-}O)_I$ and $(U{-}O)_{II}$ stretching modes and to $(U{-}O)_I$ bending vibrations respectively (800–700, ~550 and ~450 cm^{-1}) [40]. The corresponding X-ray diffraction pattern is yet poorly resolved. However, the sample heated up to 900°C clearly shows the $CuUO_4$ diffraction lines although, although some very weak reflections corresponding to CuU_3O_{10} and U_3O_8 are also present. Similar behavior was observed in the decomposition of some other natural copper and uranium compounds [41] as well as during the synthesis of these oxides from the respective copper (II) and uranium (VI) oxides [40].

Although the ESR technique seems not to be a useful tool to clarify the thermal process, some of these results are worthwhile to comment. The ESR spectrum of original sample, registered at RT show a symmetric and broad band with a g value of 2.18 ($\Delta H_{pp} \sim 300$ G). The integrated area practically corresponds to all the copper (II) present. The resolution of the ESR spectrum of a sample heated at 500° C decreases. The band is weaker and broader (~480 G). This can be attributed to the variability in the local symmetry of copper atoms or the presence of a disordered structure or a mixture of uranium and copper oxides. However, the resolution increases with temperature; the shape of the signal becomes intense at 900°C; with a g value of 2.10 and $\Delta H_{pp} = 187$ G.

On the other hand, Fig. 5a shows a SEM photograph of vandenbrandeite (surface parallel to the *c* axis (plane 001)), whereas SEM photographs 5b and c show an inclusion of triclinic crystals of kasolite (at different magnification) in a developed vandenbrandeite face.

Changes in the crystal morphology, by effect of temperature, are show in the sequence of Fig. 6 (a to d).

The morphological characteristics of the intermediate products can be directed by the water loss from the H-bonded to equatorial O atoms of the U-polyhedron. Incipient fissures parallel to the sheets (plane 001) are originated by thermal treatment from ~300°C, which evidences that the bonding across the layers is substantially weaker than the bonds within the layers and showing the cleavage parallel to the layers.

Between 500 and 700°C the morphological changes resembles those of other UOHs such as vandendriesscheite ($PbU_7O_{32}{\cdot}12H_2O$) and schoepite ($UO_3{\cdot}2H_2O$) where the loss of water is observed as a slight increase of the interlayer 001 spacing. The process leads to a separation along cleavage surfaces and the formation of gaps along grain boundary [1]. The formation of subspecies, having nearly the same metal composition as starting material has shown in these cases [1]. The presence of different type of interlayer H-bonds can be supported by the DTA and TG data [5]. Between 500 and 700°C the structural rearrangement within the layers seems to be small, because the U- and Cu-distribution within the grain boundary is homogeneous by EDAX analysis (copper content between 21 and 24%). However, the efforts to obtain crystallized samples in this range of temperature have been unsuccessful, remaining practically amorphous to XRD. Crystals morphologically different, are observed from 800°C and they are well developed from 900°C, (21.10% Cu and 78.90% U by EDAX analysis). The structural rearrangements within the sheets, as dehydration proceeds, leads to a Cu/U atomic ratio ~1, ($CuUO_4$), although a small proportion of U_3O_8 ($UO_{2.67}$ remain still at 950°C [5]). In this sense, it is interesting to notice that in a similar way to the UOHs paragenesis (determined by the crystal chemistry), the thermal decomposition path of the studied mineral seems to be also directed by the topology of structural sheets. The electron microscopy analysis allows support a topochemical process to interpret the dehydroxylation of vandenbrandeite, which is difficult to show by another technique due to the poor crystallinity of the samples. Likewise, the formation and stability of $CuUO_4$ is facilitated by the atomic arrangement in

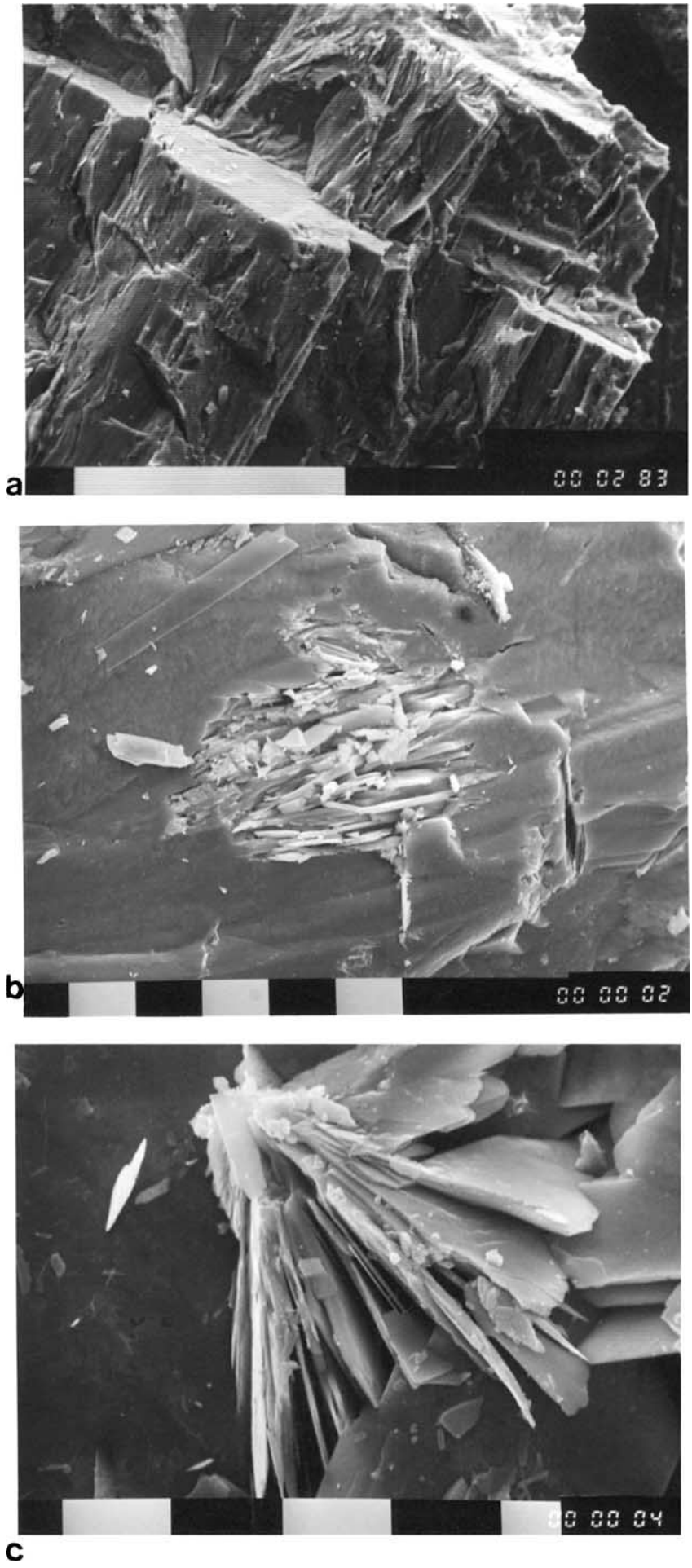

Figure 5 SEM photographs of: (a) vandenbrandeite (magnification × 500, scale bar = 100 μm); (b) kasolite inclusion at magnification × 1200, scale bar = 10 μm; (c) idem at magnification × 2000, scale bar = 10 μm.

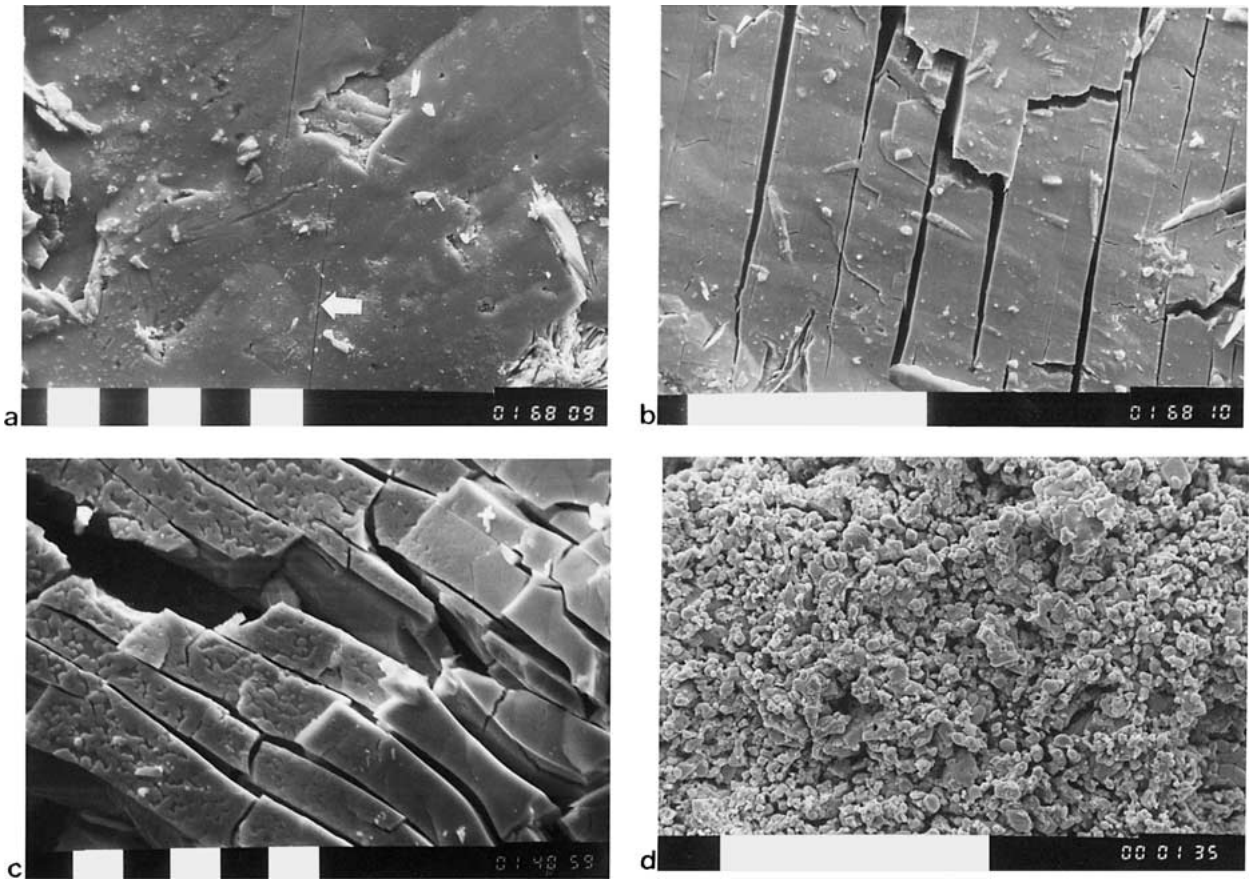

Figure 6 SEM photographs of the thermal dehydroxilation: (a) sample heated up to 300°C (magnification × 1000, scale bar = 10 μm). The arrow shows an incipient fissure; (b) sample heated at 500°C (magnification × 500, scale bar = 100 μm), (c) sample heated at 700°C (magnification × 1000, scale bar = 10 μm, (d) sample heated at 950°C (magnification × 600, scale bar = 100 μm).

the layers as well as the polarizing properties of the metallic ions.

References

1. R. J. FINCH and R. C. EWING, *J. Nucl. Mater.* **190** (1992) 133.
2. I. H. MILNE and E. W. NUFFIELD, *Amer. Mineral.* **36** (1951) 394.
3. A. ROSENWEIG and R. R. RYAN, *Cryst. Struct. Comm.* **6** (1977) 53.
4. A. SCHOEP, *Ann. Musée Congo Belge Tervuren, A, sér. 1 Minéralogie* **1** (1932) f. 3, 22.
5. J. CEJKA, *N. Jb. Miner. Mh.* **H.3** (1994) 112.
6. M. DELIENS, P. PIRET and G. COMBLAIN (Musée Royal de l'Afrique Centrale, Tervuren, 1981) 113 p.
7. V. D. C. DALTRY, *Ann. Soc. Geol. Belgique* **115** (1992) 33.
8. F. C. HAWTHORNE, *Z. Krist* **201** (1992) 183.
9. K. NAKAMOTO "Infrared and Raman Spectra of Inorganic and Coordination Compounds," 4th ed. (J. Wiley, New York, 1986).
10. V. C. FARMER, "The Infrared Spectra of Minerals" (Mineral. Soc. London, London, 1974).
11. J. HENNING, K. BECKENKAMP and H. D. LUTZ, *Appl. Spectrosc.* **44** (1990) 992.
12. A. PERRIN, Thesis, Université de Rennes, 1976, p. 210.
13. V. LORENZELLI, T. DUPUIS and J. LECOMPTE, *C. R. Acad. Sci. Paris* **259** (1964) 1057.
14. E. A. SECCO, *Can. J. Chem.* **66** (1988) 329.
15. Z. URBANEC and J. CEJKA, *Coll. Czech. Chem. Comm.* **44** (1979) 1.
16. I. L. BOTTO, *J. Less Comm. Metals* **128** (1987) 47.
17. M. M. THERESE DUPUIS, C. DUVAL and J. LECOMPTE, *C. R. Acad. Sci. Paris* **257** (1963) 3080.
18. H. D. LUTZ, *Spectrochim. Acta* **24 A** (1968) 2107.
19. H. SIEBERT, "Anwendungen der Schwingungsspektroskopie in der Anorganischen Chemie" (Springer, Berlin, Heidelberg, New York, 1966).
20. S. J. GRABOWSKI, *Croatica Chem. Acta* **63** (1990) 647.
21. G. FERRARIS and G. IVALDI, *Acta Crystallog.* **B44** (1988) 341.
22. J. CEJKA (JR), A. MUCK and J. CEJKA, *Phys. Chem. Minerals* **11** (1984) 172.
23. V. BARAN, *Coll. Czech. Chem. Comm.* **47** (1982) 1269.
24. I. L. BOTTO, E. J. BARAN and M. DELIENS, *N. Jb. Miner. Mh.* (1989) 212.
25. J. I. BULLOCK, *J. Inorg. Nucl. Chem.* **29** (1964) 2257.
26. K. OHWADA and T. SOGA, *Spectrochim. Acta* **29A** (1973) 843.
27. H. R. HOEKSTRA, *J. Inorg. Nucl. Chem.* **27** (1965) 801.
28. S. P. MCGLYNN, J. K. SMITH and W. C. NEELY, *J. Chem. Phys.* **35** (1961) 105.
29. B. W. VEAL, D. L. LAM, W. T. CARNALL and H. R. HOEKSTRA, *Phys. Rev.* **B12** (1975) 5151.
30. V. A. GLEBOB, *Koord. Khim.* **7** (1981) 388.
31. V. N. SERYOZHKIN and L. B. SERERYOZHKINA, *Zh. Neorg. Khim.* **29** (1984) 1529.
32. S. D. ROSS, "Inorganic IR and Raman Spectra" (McGraw-Hill, London, 1972).
33. K. OHWADA, *Spectrochim. Acta* **24A** (1968) 595.
34. M. PHAM THI, G. VELAZCO, PH. COLOMBAN and A. NOVAK, *Solid State Ionics* **9/10** (1983) 1055.
35. I. L. BOTTO, *Acta Sudamer. Quim.* **4** (1984) 71.
36. J. I. BULLOCK, *J. Chem. Soc. A* (1969) 781.
37. E. J. BARAN and I. L. BOTTO, *Monatsh. Chem.* **107** (1976) 633.
38. J. H. JONES, *Spectrochim. Acta* **11** (1959) 409.
39. N. I. MCDEVITT and W. L. BAUN, *ibid.* **20** (1964) 799.
40. L. N. JAKES, L. N. SEDLAKOVA, J. MORAVEC and J. GERMANIC, *J. Inorg. Nucl. Chem.* **30** (1968) 525.
41. J. CEJKA, Z. URBANEC, J. CEJKA, JR and Z. MRAZEK, *N. Jb. Miner. Abh.* **159** (1988) 297.

Received 11 July 2000
and accepted 3 August 2001